aPROMISE: A Novel Automated PROMISE Platform to Standardize Evaluation of Tumor Burden in ^{18}F-DCFPyL Images of Veterans with Prostate Cancer

Nicholas Nickols[1–4], Aseem Anand[5–7], Kerstin Johnsson[7], Johan Brynolfsson[7], Pablo Borreli[8], Neil Parikh[2], Jesus Juarez[2], Lida Jafari[9], Mattias Eiber[10], and Matthew Rettig[2,3,11]

[1]Radiation Oncology Service, VA Greater Los Angeles Healthcare System, Los Angeles, California; [2]Department of Radiation Oncology, David Geffen School of Medicine, UCLA, Los Angeles, California; [3]Department of Urology, David Geffen School of Medicine, UCLA, Los Angeles, California; [4]Institute of Urologic Oncology, Jonsson Comprehensive Cancer Center, UCLA, Los Angeles, California; [5]Department of Translational Medicine, Division of Urological Cancer, Lund University, Malmö, Sweden; [6]Department of Medicine, Memorial Sloan Kettering Cancer Center, New York, New York; [7]Department of Data Science and Machine Learning, EXINI Diagnostic AB, Lund, Sweden; [8]Department of Clinical Physiology, Sahlgrenska University Hospital, Gothenburg, Sweden; [9]Imaging Service, VA Greater Los Angeles Healthcare System, Los Angeles, California; [10]Department of Nuclear Medicine, Klinikum Rechts der Isar, Technical University of Munich, Munich, Germany; and [11]Division of Hematology-Oncology, VA Greater Los Angeles Healthcare System, Los Angeles, California

Standardized staging and quantitative reporting are necessary to demonstrate the association of ^{18}F-DCFPyL PET/CT imaging with clinical outcome. This work introduces an automated platform, aPROMISE, to implement and extend the Prostate Cancer Molecular Imaging Standardized Evaluation (PROMISE) criteria. The objective is to validate the performance of aPROMISE in staging and quantifying disease burden in patients with prostate cancer who undergo prostate-specific antigen (PSMA) imaging. **Methods:** This was a retrospective analysis of 109 veterans with intermediate- or high-risk prostate cancer who underwent PSMA imaging. To validate the performance of aPROMISE, 2 independent nuclear medicine physicians conducted aPROMISE-assisted reads, resulting in standardized reports that quantify individual lesions and stage the patients. Patients were staged as having local disease only (miN0M0), regional lymph node disease only (miN1M0), metastatic disease only (miN0M1), or both regional and distant metastatic disease (miN1M1). The staging obtained from aPROMISE-assisted reads was compared with the staging by conventional imaging. Cohen pairwise κ-agreement was used to evaluate interreader variability. Correlation coefficients and intraclass correlation coefficients were used to evaluate the inter-reader variability of the quantitative assessment (molecular imaging PSMA [miPSMA] index) at each stage. Kendall tau and t testing were used to evaluate the association of miPSMA index with prostate-specific antigen and Gleason score. **Results:** All PSMA images of 109 veterans met the DICOM conformity and the requirements for the aPROMISE analysis. Both independent aPROMISE-assisted analyses demonstrated significant upstaging in patients with localized (23%, $n = 20/87$) and regional (25%, $n = 2/8$) tumor burden. However, a significant number of patients with bone metastases identified on conventional imaging (^{18}F-NaF PET/CT) were downstaged (29%, $n = 4/14$). The comparison of the 2 independent aPROMISE-assisted reads demonstrated a high κ-agreement: 0.82 for miN0M0, 0.90 for miN1M0, and 0.77 for miN0M1. The Spearman correlation of quantitative miPSMA index was 0.93, 0.96, and 0.97, respectively. As a continuous variable, miPSMA index in the prostate was associated with risk groups defined by prostate-specific antigen and Gleason score. **Conclusion:** We demonstrated the consistency of the aPROMISE platform between readers and observed substantial upstaging in PSMA imaging compared with conventional imaging. aPROMISE may contribute to broader standardization of PSMA imaging assessment and to its clinical utility in the management of prostate cancer patients.

Key Words: ^{18}F-DCFPyL; PSMA; aPROMISE; segmentation; quantification; standardization

Prostate cancer is the most common solid tumor in men, with an incidence of nearly 192,000 cases and nearly 30,000 deaths in the United States annually. Accurate staging of a patient with prostate cancer is critical for selection of appropriate treatment strategies, especially as applied to differentiating between those with localized or regional disease who can be treated with curative intent and those with metastatic disease. Whether surgery, radiation, and systemic hormone therapy or chemotherapy are appropriate for a given patient is driven largely by the clinical stage (*1*). According to the recently updated National Comprehensive Cancer Network guidelines, ^{99m}Tc-phosphonate bone scintigraphy (bone scanning) and CT or MRI remain the standard imaging modalities for prostate cancer staging. However, bone and CT scans have demonstrated limited diagnostic accuracy in earlier disease settings (*2,3*), in turn limiting the accurate staging necessary for optimal prostate cancer management.

Accurate detection of metastatic disease is a particularly important goal because metastatic prostate cancer requires a different treatment approach and carries a significantly worse prognosis than local disease. PET is a noninvasive technique that can image bone and soft tissue in a single modality, evaluate high-grade tumors that may not produce prostate-specific antigen (PSA), and

provide quantifiable data using the SUV. However, in prostate cancer, PET tracers that image metabolic pathways, such as ^{11}C-choline, ^{11}C-acetate, and ^{18}F-FDG, suffer from suboptimal sensitivity and specificity in the detection of regional and distant metastatic disease. Recently, small ligands for PET imaging have been developed that target the cell-surface protein prostate-specific membrane antigen (PSMA), which is overexpressed in prostate cancer cells but is also expressed to some extent in other organs and blood vessels (*4*). Radiopharmaceuticals based on PSMA ligands have demonstrated high diagnostic accuracy for the detection of both regional and distant metastatic prostate cancer. The proPSMA trial demonstrated that PSMA PET/CT has greater staging accuracy than conventional imaging consisting of bone scanning and CT for initial staging of patients with high-risk prostate cancer (*5*). This supports the use of a single PSMA PET/CT scan rather than 2 conventional imaging modalities in this setting.

Recent efforts in standardizing the assessment of PSMA scans have resulted in several PSMA PET evaluation and reporting systems, including the PSMA Reporting and Data System, the system of the European Association of Nuclear Medicine, and the Prostate Cancer Molecular Imaging Standardized Evaluation (PROMISE) (*6–8*). Although all the proposed criteria are focused on the characterization of individual PSMA lesions based on the location and on the definition of significant uptake, the PROMISE standard is also proposing a patient-level staging (molecular imaging TNM), which is based on the detection and location of the disease in the PSMA PET/CT image. A recent study comparing such standardized assessments has shown that they have a high interreader reproducibility (*9,10*).

However, the adoption of PROMISE criteria in routine clinical practice and investigational studies is limited by the fact that it must be done manually and is labor-intensive. The manual work can be greatly facilitated through automation by deep-learning image analysis. The structural radiologic processes, including the segmentation of anatomic structures (from CT), can be automated to contextualize and characterize the functional imaging. The application of deep learning in automating the whole-body segmentation in PET/CT is the foundational framework for automating the PROMISE criteria. In this study, we introduce and evaluate the analysis of PSMA PET images through aPROMISE, a deep-learning platform to both automate standardized staging and generate a fully quantitative assessment of PSMA-defined disease burden at the lesion and patient levels.

MATERIALS AND METHODS

Patient Population

The purpose of our study was to evaluate the performance of the aPROMISE technology in standardizing the staging and quantification of prostate cancer. This investigation was a retrospective analysis of 109 veterans with unfavorable intermediate- and high-risk primary prostate cancer who underwent ^{18}F-DCFPyL PET/CT under clinical trial NCT03852654, a single-arm trial of PSMA PET/CT on veterans who also underwent conventional imaging with bone scanning, CT, or MRI. The study was approved by the local institutional review board at a Veterans

Affairs hospital (PCC 2018-100989), with a waiver of individual informed consent.

Study Design

To validate the performance of aPROMISE, 2 independent board-certified nuclear medicine physicians (3 y of clinical experience) reviewed the PSMA images with the assistance of aPROMISE. No prior instructions were given, and the readers solely and independently relied on the aPROMISE workflow. aPROMISE provides the reader with automated segmentation and quantification of lesions with a pre-selected molecular imaging TNM type. The reader can choose to accept or override the aPROMISE automated selections at the level of each individual lesion. A final report is autogenerated on the basis of the aPROMISE-assisted read.

First, the aPROMISE-assisted staging was evaluated against conventional-imaging staging obtained from the routine clinical reports. Conventional imaging in every patient included ^{99m}Tc-methylene diphosphonate bone scanning or ^{18}F-NaF PET/CT, and CT or MRI of the pelvis. Second, we evaluated the reproducibility of the staging and lesion quantification between the 2 independent aPROMISE-assisted reads. Finally, we evaluated the clinical association of quantitative PSMA uptake (molecular imaging PSMA [miPSMA] index) with 2 baseline clinical variables: Gleason score and PSA value. All patients were staged into 1 of 4 distinct categories: miN0M0 (localized disease and absence of regional lymph node or distant metastatic disease), miN1M0 (regional lymph node disease but absence of distant metastatic disease), miN0M1 (absence of regional lymph node but presence of distant metastatic disease), and miN1M1 (presence of both regional lymph node and distant metastatic disease).

aPROMISE and miPSMA Index

aPROMISE (version 1.1), a class II software as a medical device, is a web application developed by EXINI Diagnostics AB to standardize and quantify PSMA imaging in prostate cancer. aPROMISE is enabled with deep learning that automatically analyzes the CT image to segment anatomic regions in detail, including individual vertebrae, ribs, pelvic bones, and soft-tissue organs such as the prostate (Fig. 1). The anatomic contextualization of the molecular image is used to stage the patient on the basis of the location and extent of the primary tumor in the prostate and of the disease in the local or regional pelvic lymph nodes and in the distant metastases. Subsequently, the PET image is analyzed to detect target lesions. aPROMISE technology enables implementation of standard guidelines such as PROMISE in
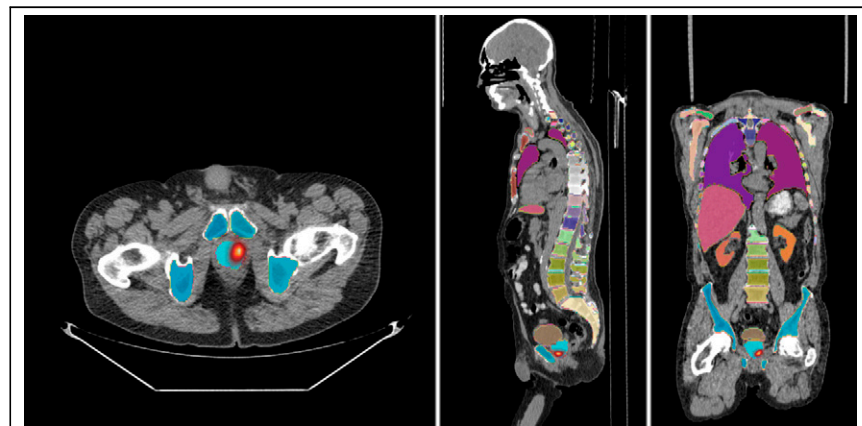
FIGURE 1. Deep-learning–enabled segmentation of anatomic context in low-dose CT component of PET/CT. Individual color represents respective segmented organ. aPROMISE technology enables automated segmentation of reference organs and anatomic delineation of disease in prostate tumor, regional lymph node, and distant metastases.

standardizing PSMA assessment (6). Merging the target lesion information with the anatomic location, the technology quantifies each target lesion in terms of both intensity and volume and summarizes by tissue type to generate the miPSMA index. The aPROMISE report is created automatically, with both aggregated information and detailed information on a per-lesion basis. Manual controls are provided as fallback to augment automatic analysis.

In the PROMISE criteria, Eiber et al. (6) defined the miPSMA score of a lesion as 0 when uptake is below the level in the aorta, 1 when uptake is between the levels in the aorta and liver, 2 when uptake is between the levels in the liver and the parotid gland, and 3 when uptake is above the level in the parotid gland. The miPSMA lesion index is a continuous extension of these criteria, defined by linear interpolation from the lesion SUV_{mean} and from the aorta and liver SUV references as follows:

$$\text{Lesion } SUV_{mean} \leq \text{aorta } SUV_{ref}:$$
$$\text{Lesion index} = \frac{\text{lesion } SUV_{mean}}{\text{aorta } SUV_{ref}}$$
$$\text{Aorta } SUV_{ref} \leq \text{lesion } SUV_{mean} \leq \text{liver } SUV_{ref}:$$
$$\text{Lesion index} = 1 + \frac{\text{lesion } SUV_{mean} - \text{aorta } SUV_{ref}}{\text{aorta } SUV_{ref}}$$
$$\text{Liver } SUV_{ref} \leq \text{lesion } SUV_{mean} \leq 2 \times \text{liver } SUV_{ref}:$$
$$\text{Lesion index} = 2 + \frac{\text{lesion } SUV_{mean} - \text{liver } SUV_{ref}}{\text{liver } SUV_{ref}}$$
$$2 \times \text{liver } SUV_{ref} \leq \text{lesion } SUV_{mean}: \text{lesion index} = 3.$$

The use of the parotid gland as a threshold has been replaced by 2 times the liver reference since it is not certain that the parotid glands are included in all PSMA PET/CT scans. For each molecular imaging TNM type, lesion uptake is aggregated into the intensity-weighted total lesion uptake volume. This PSMA index is defined as

$$\sum_{\text{lesion type}} \text{lesion index} \times \text{lesion uptake volume}$$

for extent of disease in any lesion type (primary tumor [T stage], local or regional pelvic nodes [N stage], or distant metastases [M stage, which is further denoted as "a" for metastatic lymph nodes, "b" for bone metastases, and "c" for visceral organ metastases]).

Statistical Analysis

Descriptive statistics were used to compare the aPROMISE staging with conventional-imaging staging. Cohen pairwise κ-agreement was used to evaluate the interreader variability of aPROMISE-assisted staging (miN0M0, miN1M0, and miN0M1). Spearman and Kendall correlation coefficients were used to evaluate the interreader variability of the quantitative assessment (miPSMA index) of each stage. Student t testing was used to evaluate the miPSMA index values (in tumor) in the risk groups defined by PSA and Gleason score. All statistical analyses were performed using R, version 4.0.2.

RESULTS

The analysis included 109 consecutive patients, whose baseline characteristics are detailed in Table 1. Conventional imaging staged 87 of the 109 patients as having N0M0 disease, 8 patients as having N1M0 disease, 14 patients as having N0M1 disease, and no patients as having N1M1 disease. All 14 of the N0M1 patients were found to have bone metastasis (N0M1b) on conventional staging by ^{18}F-NaF PET/CT and did not undergo ^{99m}Tc-methylene diphosphonate bone scanning.

The duration of the aPROMISE-assisted read, from selecting a patient to generating a complete report, was recorded to be a mean of 3.2 min (range, 1.8–5.1 min) per scan for reader 1 and 3.4 min (range, 2.3–5.8 min) for reader 2. The comparative assessment of conventional against aPROMISE-assisted PSMA staging is detailed in Table 2. Both aPROMISE-assisted PSMA analyses demonstrated significant upstaging in patients with localized and regional tumor burden and downstaging in patients who were positive for distant bone metastasis by ^{18}F-NaF PET/CT. In aPROMISE-assisted read 1, of the 87 patients who were determined to be negative for local (N1) or distant (M1) metastatic disease by conventional imaging, 20 (23%) were upstaged in the PSMA imaging assessment to having regional lymph node disease ($n = 13$) or distant metastatic disease ($n = 6$). Similarly, of the 8 patients staged as having local pelvic nodal disease only (N1), 2 (25%) were upstaged to having distant metastatic disease also. Notably, a significant population (4/14, 29%) with bone metastatic disease by conventional imaging were downstaged by aPROMISE-assisted PSMA imaging. Examples of downstaged aPROMISE-assisted PSMA reads against ^{18}F-NaF reads are

TABLE 1
Patient Characteristics ($n = 109$)

Characteristic	Data
Age (y)	
Average	70
Median	69
Minimum	55
Maximum	86
Race (n)	
White	54 (49%)
African American	44 (41%)
Hispanic	7 (7%)
Asian Pacific Islander	3 (2%)
Native American	1 (1%)
Clinical T stage (n)	
cT1/2	62 (57%)
cT3	47 (43%)
Gleason score (n)	
3 + 3	13 (7%)
3 + 4	28 (23%)
4 + 3	24 (18%)
≥4 + 4	49 (36%)
PSA at diagnosis (ng/mL)	
Average	20.4 ng/mL
Median	13.55 ng/mL
Minimum	3.03 ng/mL
Maximum	167.92 ng/mL
Percentage positive core (n)	
<25%	18 (17%)
25%–50%	28 (26%)
51%–75%	14 (13%)
>75%	28 (26%)
Unknown	11 (10%)

TABLE 2
aPROMISE-PSMA Staging Reads vs. Local and Distant Metastatic Staging by Conventional Imaging

Read no.	Parameter	Conventional imaging			
		N0M0 ($n = 87$)	N1M0 ($n = 8$)	N0M1a/b ($n = 14$)	N1M1a/b ($n = 0$)
1	miN0M0 ($n = 71$)	67	0	4	0
	miN1M0 ($n = 19$)	13	6	0	0
	miN0 M1a/b ($n = 15$)	6	0	9	0
	miN1M1a/b ($n = 4$)	1	2	1	0
2	miN0M0 ($n = 72$)	68	0	4	0
	miN1M0 ($n = 18$)	12	6	0	0
	miN0M1a/b ($n = 15$)	6	0	9	0
	miN1M1a/b ($n = 4$)	1	2	1	0

$n = 109$.

demonstrated in Figure 2. aPROMISE-assisted read 2 had observations similar to those on conventional imaging (Table 2).

Interobserver Reproducibility of aPROMISE Reads

The 2 independent aPROMISE-assisted read are compared in Table 3. The κ-agreement between them was 0.82 for categorization of patients with miN0M0, 0.90 for patient with miN1M0, and 0.77 for patients with miN0M1b. Among all stages, the relatively

FIGURE 2. Example of patients who were negative in aPROMISE-assisted reads of ^{18}F-DCFPyL scans (A and C, axial images) compared with Na^{18}F (B and D, axial images) and were downstaged from N0M1 to N0M0.

modest discrepancy in aPROMISE-associated reads was most notable for isolated low-intensity bone lesions. The quantitative reproducibility of miPSMA index in the cases that were categorized the same in the 2 independent aPROMISE-assisted reads—miN0M0 ($n = 66$), miN1M0 ($n = 17$), miN0M1($n = 12$)—is illustrated in Figure 3. The Spearman correlation was 0.93, 0.96, and 0.97, respectively.
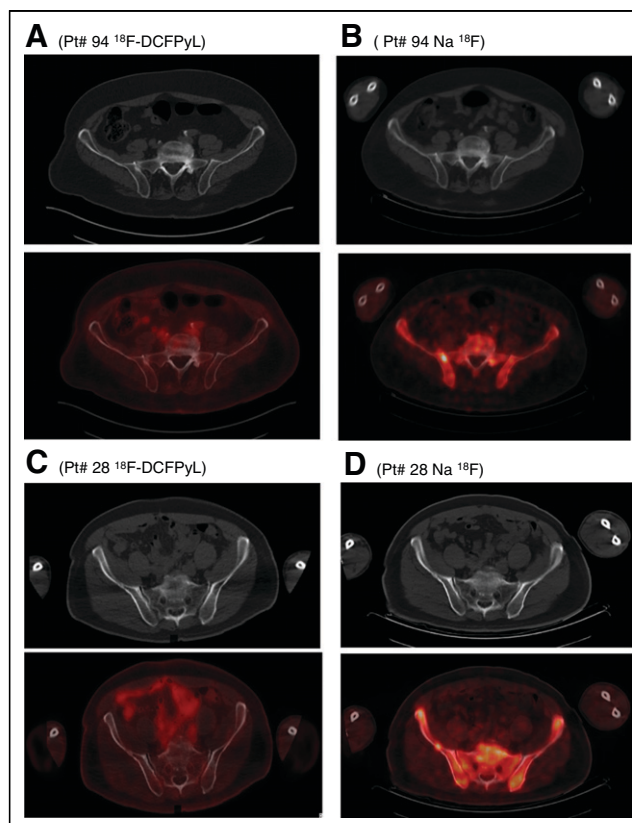
aPROMISE miPSMA Index

As a continuous variable, miPSMA index in the prostate tumor of all patients ($n = 109$) was correlated with PSA value ($t = 0.30$; $P < 0.0001$). Figure 4 shows the miPSMA index values in the prostate, stratified in risk groups defined by PSA and separately by Gleason score. There was a significant difference in values between patients with a PSA of 10 ng/mL or lower (median, 17.61; interquartile range, 8.75–44.63) and patients with a PSA of 20 ng/mL or higher (median, 54.63; interquartile range, 27.55–80.79) ($P = 0.05$). Similarly, the PSMA index values of prostate tumors with a Gleason score of $3 + 3$ (median, 19.45; interquartile range, 9.97–23.54) was significantly lower than that of tumors with a Gleason score of at least $4 + 3$ (median, 32.74; interquartile range, 15.38–54.63) ($P = 0.01$).

DISCUSSION

The aPROMISE-assisted independent staging and the quantitative assessments of total disease burden were found to be consistent and reproducible between readers. Integrating PSMA assessment tools into the clinical workflow could allow for automation to provide efficiency, consistency, and accuracy in the staging and quantification of PSMA PET/CT. This study also demonstrated that aPROMISE-assisted reads for PSMA PET/CT detected significantly more regional and metastatic suggestive lesions than were identified by conventional imaging.

The ability of PSMA imaging to detect a greater number of suspected metastatic lesions than can be detected by conventional bone scanning or CT has been evident across multiple studies ([11–14]). The frequency of upstaging in nodal and distant metastasis by PSMA PET/CT, compared with conventional imaging, in this cohort of patients with intermediate- or high-risk prostate cancer was in line with previous reports. Notably, the biologic

TABLE 3
Local and Distant Metastatic Staging by aPROMISE-PSMA Read 1 Against aPROMISE-PSMA Read 2

| | Read 1 | | | |
Read 2	miN0M0 ($n = 71$)	miN1M0 ($n = 19$)	miN0M1a/b ($n = 15$)	miN1M1a/b ($n = 4$)
miN0M0 ($n = 72$)	67	2	3	0
miN1M0 ($n = 18$)	1	17	0	0
miN0M1a/b ($n = 15$)	3	0	12	0
miN1M1a/b ($n = 4$)	0	0	0	4

$n = 109$.

dimension of PSMA in evaluating suspected metastatic disease was particularly apparent when comparing findings from ^{18}F-NaF with those from PSMA imaging. Of the 14 patients categorized as M1b through ^{18}F-NaF scans, 4 (29%) were called negative in aPROMISE-assisted reads of their respective PSMA scans. As a bone metabolic scan, ^{18}F-NaF imaging is known to be susceptible to nonpathophysiologic features in bone such as trauma, degenerative changes, and fibrous dysplasia. Of these 4 patients with lesions seen on ^{18}F-NaF imaging but not on PSMA PET/CT, 2 demonstrated lesions that appeared more likely to be benign on PSMA PET/CT but were called positive on the corresponding ^{18}F-NaF imaging. The other 2 patients with discordant findings between ^{18}F-NaF and PSMA imaging had suggestive sclerotic bone lesions that were not seen on the aPROMISE reads because of low PSMA intensity in the lesions. One of these 2 patients underwent curative-intent radical prostatectomy and remains free of biochemical recurrence almost 1 y after surgery, without additional therapy. The other patients delayed treatment and instead underwent a repeat ^{18}F-NaF examination 6 mo later that showed no interval change in the bone lesion but did show progression within soft tissue. In these 2 cases, clinical follow-up was more consistent with the PSMA PET staging than with the ^{18}F-NaF imaging. A more comprehensive comparison of PSMA and ^{18}F-NaF imaging is beyond the scope of this study but will be done in a separate follow-up analysis.

Interreader agreement on the interpretation of PSMA PET/CT has been evaluated mostly using ^{68}Ga-PSMA11 PET/CT. Fendler et al. evaluated interreader agreements in 50 patients with primary disease and after biochemical recurrence and found κ values of 0.62 for primary tumor, 0.74 for nodes, and 0.88 for bone lesions (15). In a more homogeneous biochemically recurrent population consisting of patients with PSA levels of up to 0.6 ng/mL, Miksch et al. demonstrated κ values of 0.76 for primary tumor, 0.73 for nodes, and 0.58 for bone lesions (16). In a study focused exclusively on 50 patients who underwent ^{18}F-DCFPyL PET, an intraclass correlation coefficient of 0.79 was derived for nodal disease (17). Similarly, the manual reproducibility of following the PROMISE classification has been reviewed and reported by Toriihara et al., who demonstrated moderate interreader agreement (0.67) for molecular imaging TNM classification in PSMA PET/CT (9). The agreement between the aPROMISE-assisted reads in our study compares favorably against these prior evaluations (Cohen κ > 0.75), with a notably quick reading time (mean, 3.2 and 3.4 min per scan). One reader in our study had considerably more prior experience in the interpretation of PSMA PET/CT than

did the other. Still, a high degree of agreement was noted. The readers in our study did not get any strict guidance on lesion detection, nor did they receive any formal training on the PROMISE criteria. The findings may suggest that an aPROMISE-assisted read that involves automated segmentation, localization, and lesion preselection may nudge readers toward a moderately high agreement irrespective of their prior experience. This hypothesis warrants a multicenter, multireader study for validation.

Quantitative metrics of disease burden may further enhance the prognostic and predictive power of imaging. Currently, the automated bone scan index (aBSI) is the only Food and Drug Administration–cleared software as a medical device that has been prospectively validated in a registration study as a prognostic imaging biomarker for metastatic prostate cancer (18). The STAMPEDE trial investigated the addition of radiation to the primary tumor in M1 patients. In a post hoc analysis that used aBSI to assess disease burden, aBSI was predictive of response to prostate radiotherapy (19). aBSI uses a machine-learning algorithm that preselects and segments the lesions in bone and automatically computes a quantitative total tumor burden in ^{99m}Tc planar bone scans (20). In some sense, the miPSMA index for quantification of disease burden defined by PSMA PET/CT can be considered a 3-dimensional analog of aBSI.

However, the automated miPSMA index offers a far more comprehensive assessment of disease burden. The miPSMA index is a continuous extension of the miPSMA score proposed in the PROMISE criteria. Like the miPSMA score, the miPSMA index is the PSMA quantification of an individual lesion in relation to the mean uptake in reference organs. The result, for each lesion, is a linear PSMA-burden quantification that can be summarized by each tissue type (primary tumor [T stage], local or regional pelvic nodes [N stage], or distant metastases [M stage, which is further denoted as "a" for metastatic lymph nodes, "b" for bone metastases, and "c" for visceral organ metastases]). Our study showed an association between miPSMA index in the primary tumor and both Gleason grade and PSA value. This finding is consistent with prior studies reporting that PSMA expression in the primary tumor is associated with a higher Gleason grade and recurrence risk (21,22). We hypothesize that the miPSMA index may be useful for selecting patients for PSMA-targeted radiotherapy, with current trials largely using qualitative assessments of PSMA expression as inclusion criteria. Moreover, there is a potential role for the miPSMA index in conjunction with morphologic findings as a quantitative method of response assessment after treatment.

The purpose of our hypothesis-generating study was to evaluate the performance of the aPROMISE technology for subsequent
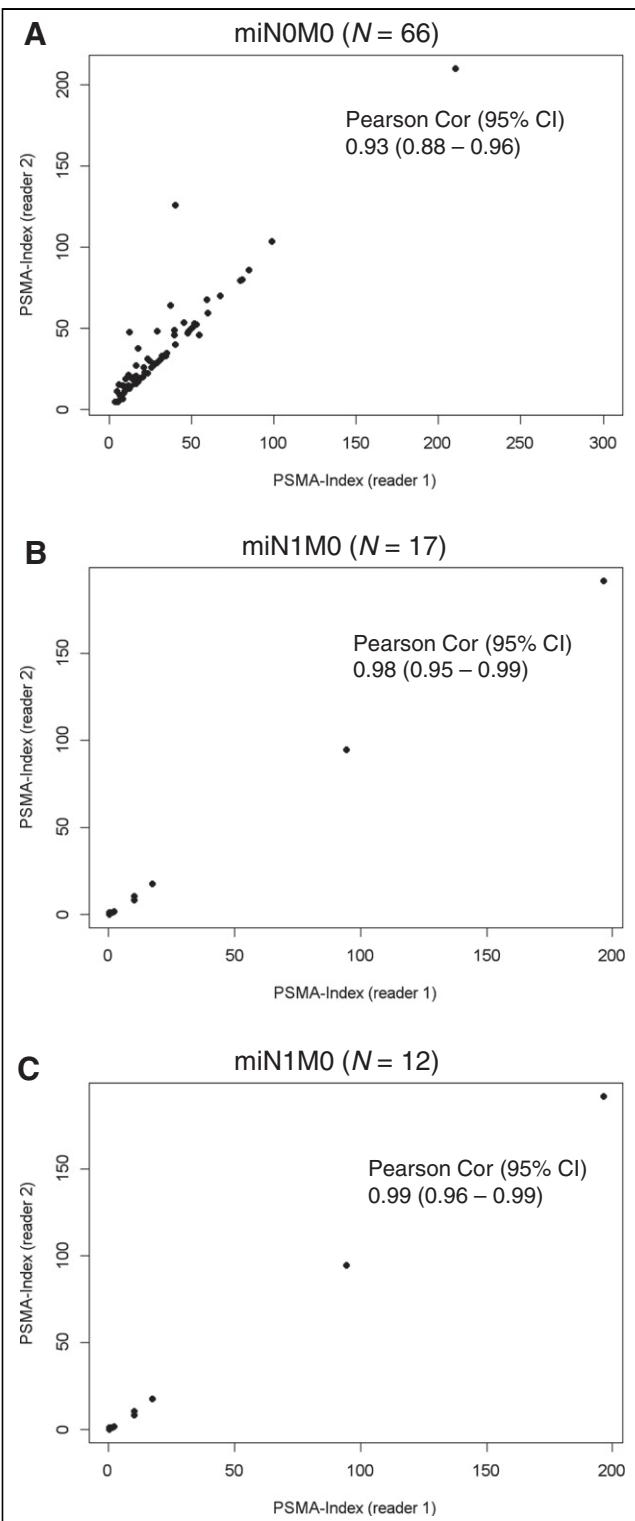
FIGURE 3. Quantitative reproducibility of miPSMA index in patients who were categorized the same in 2 independent aPROMISE-assisted reads: miN0M0 (A), miN1M0 (B), and miN0M1(C). In A, 1 patient was excluded because of a manual segmentation error that incorporated bladder. Cor = correlation.

whether the diagnostic performance of PSMA PET/CT is enhanced when using the aPROMISE software. Our study was limited in the number of independent reads and in its retrospective design. Therefore, the findings and the hypothesis presented here should be validated in a prospectively designed multireader and multiinstitutional
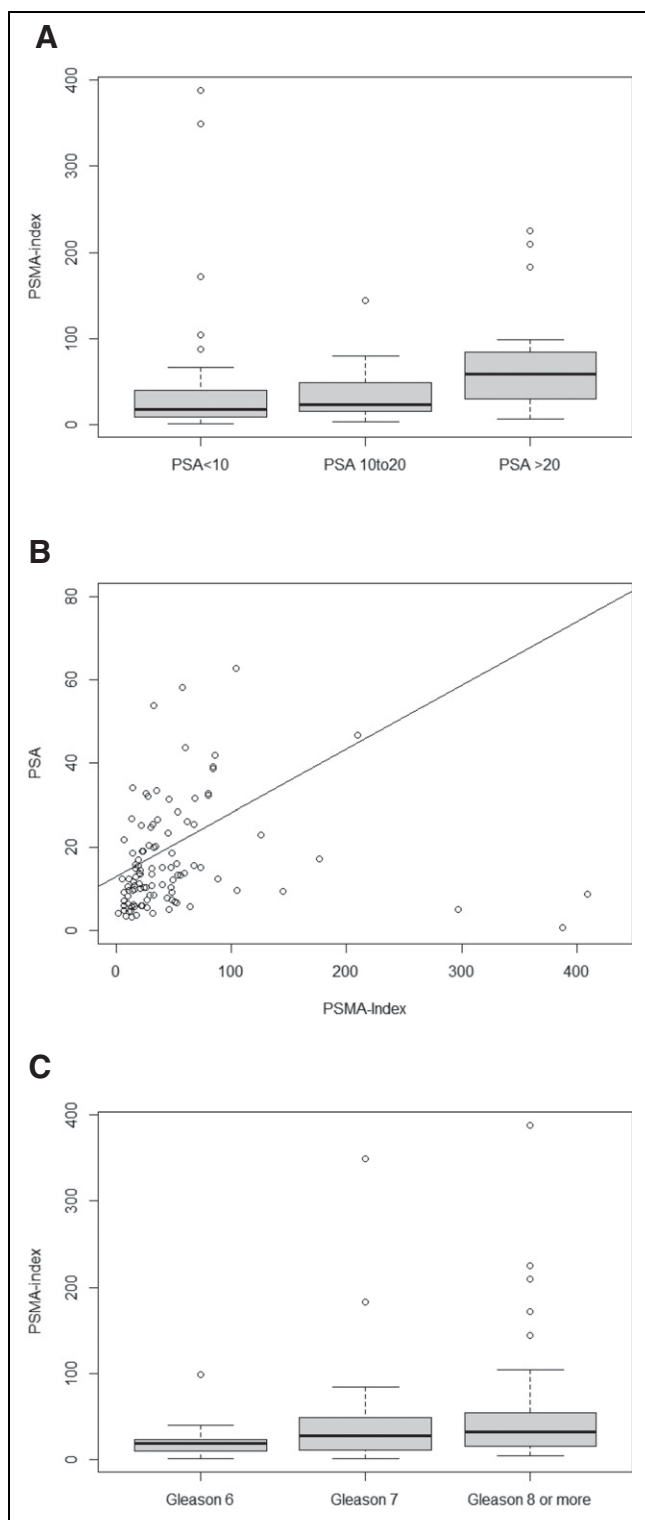
FIGURE 4. miPSMA index values in prostate, stratified by PSA (A and B) and separately by Gleason grade (C).

prospective clinical investigations. The findings here enable future investigations to evaluate any additive benefits of aPROMISE-assisted reads over manual reads of PSMA PET/CT and to assess

study design. In addition, lesions selected by aPROMISE have not been histopathologically validated. However, PSMA PET was shown to have high specificity in several recent studies (*23*).

Despite these limitations, our study demonstrated the performance of aPROMISE in an independent assessment. Incorporation of aPROMISE and the miPSMA index into subsequent clinical investigations can allow further exploration of the clinical context of their use for prospective validation.

CONCLUSION

aPROMISE-assisted PSMA PET/CT reads generate detailed imaging reports at the whole-patient and lesion levels within minutes. Compared with conventional imaging, aPROMISE assistance upstages patients and reduces interreader variability, even among readers with differing baseline levels of experience. Moreover, aPROMISE-assisted reads may standardize PSMA evaluation. Prospective studies and direct manual comparison studies are required to validate these findings. The miPSMA index is a quantitative measure of lesion volume and relative intensity, is associated with Gleason grade and PSA, and describes overall and tissue-specific tumor burden. Evaluation of the miPSMA index as an imaging biomarker of disease burden is warranted in order to assess prognostic value.

DISCLOSURE

KEY POINTS

QUESTION: Can the aPROMISE platform generate a consistent and standardized evaluation of PSMA scans?

PERTINENT FINDINGS: The comparison of the 2 independent aPROMISE-assisted reads demonstrated a high κ agreement in staging of patients. As a continuous variable, miPSMA index in the prostate was associated with risk groups defined by PSA values and Gleason scores.

IMPLICATIONS FOR PATIENT CARE: aPROMISE-assisted reads may standardize PSMA evaluation and reduce interreader variability, even among readers with differing baseline levels of experience. The miPSMA index is a quantitative measure of lesion volume and relative intensity, is associated with Gleason grade and PSA, and describes overall and tissue-specific tumor burden.

REFERENCES

1. Mohler JL, Antonarakis ES, Armstrong AJ, et al. Prostate cancer, version 2.2019, NCCN clinical practice guidelines in oncology. *J Natl Compr Canc Netw.* 2019; 17:479–505.
2. Abuzallouf S, Dayes I, Lukka H. Baseline staging of newly diagnosed prostate cancer: a summary of the literature. *J Urol.* 2004;171:2122–2127.
3. Golimbu M, Morales P, Al-Askari S, Shulman Y. CAT scanning in staging of prostatic cancer. *Urology.* 1981;18:305–308.
4. Budäus L, Leyh-Bannurah SR, Salomon G, et al. Initial experience of 68Ga-PSMA PET/CT imaging in high-risk prostate cancer patients prior to radical prostatectomy. *Eur Urol.* 2016;69:393–396.
5. Hofman MS, Lawrentschuk N, Francis RJ, et al. Prostate-specific membrane antigen PET-CT in patients with high-risk prostate cancer before curative-intent surgery or radiotherapy (proPSMA): a prospective, randomised, multicentre study. *Lancet.* 2020;395:1208–1216.
6. Eiber M, Herrmann K, Calais J, et al. Prostate Cancer Molecular Imaging Standardized Evaluation (PROMISE): proposed miTNM classification for the interpretation of PSMA-ligand PET/CT. *J Nucl Med.* 2018;59:469–478.
7. Fanti S, Minozzi S, Morigi JJ, et al. Development of standardized image interpretation for 68Ga-PSMA PET/CT to detect prostate cancer recurrent lesions. *Eur J Nucl Med Mol Imaging.* 2017;44:1622–1635.
8. Rowe SP, Pienta KJ, Pomper MG, Gorin MA. PSMA-RADS version 1.0: a step towards standardizing the interpretation and reporting of PSMA-targeted PET imaging studies. *Eur Urol.* 2018;73:485–487.
9. Toriihara A, Nobashi T, Baratto L, et al. Comparison of 3 interpretation criteria for 68Ga-PSMA11 PET based on inter- and intrareader agreement. *J Nucl Med.* 2020; 61:533–539.
10. Demirci E, Akyel R, Caner B, et al. Interobserver and intraobserver agreement on prostate-specific membrane antigen PET/CT images according to the miTNM and PSMA-RADS criteria. *Nucl Med Commun.* 2020;41:759–767.
11. Calais J, Czernin J, Cao M, et al. 68Ga-PSMA-11 PET/CT mapping of prostate cancer biochemical recurrence after radical prostatectomy in 270 patients with a PSA level of less than 1.0 ng/mL: impact on salvage radiotherapy planning. *J Nucl Med.* 2018;59:230–237.
12. Calais J, Kishan AU, Cao M, et al. Potential impact of 68Ga-PSMA-11 PET/CT on the planning of definitive radiation therapy for prostate cancer. *J Nucl Med.* 2018; 59:1714–1721.
13. Maurer T, Gschwend JE, Rauscher I, et al. Diagnostic efficacy of 68gallium-PSMA positron emission tomography compared to conventional imaging for lymph node staging of 130 consecutive patients with intermediate to high risk prostate cancer. *J Urol.* 2016;195:1436–1443.
14. van Leeuwen PJ, Emmett L, Ho B, et al. Prospective evaluation of 68gallium-prostate-specific membrane antigen positron emission tomography/computed tomography for preoperative lymph node staging in prostate cancer. *BJU Int.* 2017;119: 209–215.
15. Fendler WP, Calais J, Allen-Auerbach M, et al. 68Ga-PSMA-11 PET/CT interobserver agreement for prostate cancer assessments: an international multicenter prospective study. *J Nucl Med.* 2017;58:1617–1623.
16. Miksch J, Bottke D, Krohn T, et al. Interobserver variability, detection rate, and lesion patterns of 68Ga-PSMA-11-PET/CT in early-stage biochemical recurrence of prostate cancer after radical prostatectomy. *Eur J Nucl Med Mol Imaging.* 2020; 47:2339–2347.
17. Werner RA, Bundschuh RA, Bundschuh L, et al. Interobserver agreement for the standardized reporting system PSMA-RADS 1.0 on 18F-DCFPyL PET/CT imaging. *J Nucl Med.* 2018;59:1857–1864.
18. Armstrong AJ, Anand A, Edenbrandt L, et al. Phase 3 assessment of the automated bone scan index as a prognostic imaging biomarker of overall survival in men with metastatic castration-resistant prostate cancer: a secondary analysis of a randomized clinical trial. *JAMA Oncol.* 2018;4:944–951.
19. Ali A, Hoyle AP, Parker CC, et al. The automated bone scan index as a predictor of response to prostate radiotherapy in men with newly diagnosed metastatic prostate cancer: an exploratory analysis of STAMPEDE's "M1|RT comparison." *Eur Urol Oncol.* 2020;3:412–419.
20. Ulmert D, Kaboteh R, Fox JJ, et al. A novel automated platform for quantifying the extent of skeletal tumour involvement in prostate cancer patients using the bone scan index. *Eur Urol.* 2012;62:78–84.
21. Hupe MC, Philippi C, Roth D, et al. Expression of prostate-specific membrane antigen (PSMA) on biopsies is an independent risk stratifier of prostate cancer patients at time of initial diagnosis. *Front Oncol.* 2018;8:623.
22. Demirci E, Kabasakal L, Sahin OE, et al. Can SUVmax values of Ga-68-PSMA PET/CT scan predict the clinically significant prostate cancer? *Nucl Med Commun.* 2019;40:86–91.
23. Pienta KJ, Gorin MA, Rowe SP, et al. A phase 2/3 prospective multicenter study of the diagnostic accuracy of prostate specific membrane antigen PET/CT with 18F-DCFPyL in prostate cancer patients (OSPREY). *J Urol.* 2021;206:52.